ACADEMIA ROMÂNĂ
Revue Roumaine de Chimie
http://web.icf.ro/rrch/

Rev. Roum. Chim.,
2011, *56*(2), 115-128

ADSORPTION AND INHIBITIVE CORROSION PROPERTIES OF SOME NEW POLYMERIC COMPOUNDS ON CARBON STEELS IN COOLING WATER SYSTEMS

Florina BRÂNZOI[a], Viorel BRÂNZOI[b*], and Iulia HĂRĂBOR[b]

[a]Institute of Physical Chemistry, 202 Splaiul Independenței, Bucharest - 060021, Roumania,
E-mail fbrinzoi@chimfiz.icf.ro
[b]University Politehnica of Bucharest, 132 Calea Griviței, Bucharest - 010737, Roumania,
E-mail iv_branzoi@chim.upb.ro

Received June 4, 2010

Using the microwaves energy new organic polymers were synthesised by radicalic polymerization. These new organic compounds have anticorrosive and antiscale properties and for this reason, were used for cooling water systems protection. The inhibition activity analysis of these new organic polymers was made by assuming that the mechanism of inhibition by organic molecules is chemisorptions and that the energetic of the corrosion process per se is unaffected by the addition of substituents on the parent compound. We presume that, these new organic polymers inhibit corrosion of carbon steel by a protective mechanism, forming insoluble iron complexes and repairing the porous oxide layers. The methods employed were potentiodynamic polarization, electrochemical impedance spectroscopy and metallurgical microscopy techniques. The addition of the organic inhibitors led in all the cases to inhibition of the corrosion rate. The inhibition efficiency was high in all the studies cases. The corrosion parameters obtained from polarization curves and from EIS spectra are in good concordance and point out the inhibitory action of these new organic polymers. The adsorptions of the organic compounds on the carbon steels surface obeyed Langmuir's isotherm. Using Fourier transform infrared spectroscopy (FT-IR) it was proved the adsorption of organic inhibitors and the formation of corrosion products on the carbon steels surface

INTRODUCTION

Metal corrosion in water-conveying systems such as cooling water circuits is of major concern in industrial applications. It is well known that, in all the cases of cooling water systems at the metal/water surface contact appear frequent corrosion processes which determine deposition of corrosion products, like scales. Due to these scales formation the exchange heat becomes more difficult, fact that disturbs the normal function of industrial installation. In order to decrease corrosion of pipes, heat exchangers etc. corrosion inhibitors are widely applied. In this regard, aspects like cost of treatment versus cost of corrosion damages as well as process safety and the impact of corrosion and corrosion treatment on the environment have to be taken into account. It is well known that, excessive corrosion does not only lead to serious damage of installations, it also causes considerable environmental pollution with heavy metals. State-of-the art corrosion inhibiting products provide satisfying performance using zinc salts, molybdates, phosphate and phosphonates. Frequently, such inhibitors are discharged to the environment without further treatment. Zinc and molybdenum represent heavy metals; phosphate and phosphonates (which are eventually converted into phosphates) contribute to the nutrification of surface water. Furthermore, most of the common phosphonates are classified as poorly biodegradable. Consequently, an objective is to develop low-toxic, heavy metal and phosphorus free corrosion inhibitors with good biodegradability. For this reason, corrosion

* Corresponding author: iv_branzoi@chim.upb.ro

inhibiting systems based on different carboxylic acids have been developed which achieve an inhibition efficiency comparable to state –of- the art phosphonic acid based systems while additionally providing enhanced environmental compatibility and biodegradability. Some organic compounds are effective corrosion inhibitors. Most previous research into their usage has concentrated on relationships between chemical structure and inhibition performance. Recent investigations have additionally emphasized the importance of the nature of the metal surface in inhibition performance.[1]The ability of an inhibitor to provide corrosion protection therefore depends to a large extent upon the interaction between the inhibitor and the metal surface under corrosion conditions. Generally, it is assumed that strong adsorption of the inhibitors is a prerequisite. The adsorption of inhibitors leads to the formation of a physical barrier that reduces the metal reactivity in the electrochemical reaction of corrosion .[2] Early studies considered the adsorption of inhibitors on metal surfaces to be primarily physical adsorption and/or chemisorptions.[3-6, 9-11] New investigations have shown that adsorption could also occur through hydrogen bonding.[1, 7-8] Most of these studies made use of sensitive surface analysis tools such as X-ray photoelectron spectroscopy (XPS) to resolve the nature of inhibitor adsorption.[13-17] Some earlier work has however been carried out under conditions that are not representative of on actual application.[18-22] The validity of the conclusions derived from such idealized experiments in actual practice remains an open question. In this paper, the inhibition of mild steel corrosion in cooling waters by organic compounds was investigated by potentiodynamic polarizations, EIS measurements and metallography analysis. This paper presents some attempts of analyzing of corrosive phenomena, which occur in cooling water systems, and relates to the protection of metallic surfaces from corrosion using these new polymers obtained in microwaves field.

EXPERIMENTAL

The inhibitory action was studied through tracing the polarization curves obtained using the, potentiodynamic method calculation of the kinetic parameters of corrosion in case of solutions with inhibitors, especially the corrosion current densities, and their comparison with the kinetic parameters of the solution without inhibitors. The polarization curves were obtained by potentiostatic and potentiodynamic methods. In all experiments the electrochemical polarizations were started about 30 minutes after the working electrode was immersed in solution, to allow the stabilization of the stationary potential. The working electrode potential was always measured with reference to the saturated calomel electrode and was plotted against current from external circuit, obtaining the anodic or cathodic curves according to the variation of the working electrode potential. In order to reduce the ohmic resistance, we used a single compartment cell in which the working electrode was situated in the cell center and surrounded by the auxiliary electrode made of bright platinum gauze. The studied metals were the carbon steels type OL 37 and OLC 45.

The used organic inhibitors were three polymers, which were obtained by radicalic polymerization in presence of microwave field: PASAC-1 (maleic anhydride and urea molar ratio 1.5:1 at t=140^{o}C), PASP-polyaspartic acid, and PASAC-2 (polyaspartic acid and phosphoric acid molar ratio 1:0.1at t=160^{o}C),

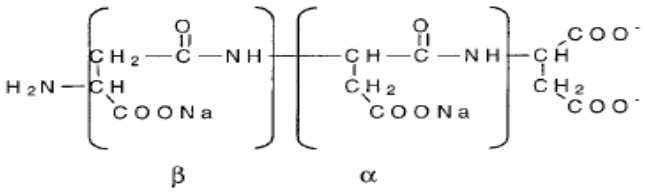

(1)

The chemical compositions of the studied metallic materials are given in the tables 1.

Table 1

The chemical composition of the working electrodes

Electrode	C%	Si%	Mn%	Fe%	P%	S%	Al%	Ni%	Cr%	Cu%	Sn%	As%
OLC 45	0.48	0.03	0.79	98.32	0.02	0.025	0.027	0.05	0.06	0.18	0.012	0.006
OL 37	0.15	0.09	0.4	99.293	0.023	0.02	0.022	0.001	0.001	-	-	-

The working electrode was made from these metallic materials and had a cylindrical shape. This shape is preferred, because it assures a greater surface and a reduce number of edges. Prior to each determination, the working electrode was mechanically ground and polished with emery paper of varied granulation up to mirror-luster, degreased in benzene at

boiling temperature in order to remove all traced of fat and remained abrasive powder on the electrode surface after polishing. After that, the working electrode was washed with distilled water and inserted in the polarization cell, which was the usually three-electrode cell. All tests have been performed at 25°C under atmospheric oxygen without agitation. The electrochemical measurements were made using an automated model VoltaLab 40 potentiostat/galvanostat. Surface analysis on the carbon steel electrode of the formed adsorbed film was accomplished by both FT-IR (FT-IR spectrometer Bruker optik) and metallographic micrographies (Hund H660).

The corrosion medium was industrial cooling water with the following chemical composition:

Table 2

The chemical composition of the cooling water type SC_1

Indicators	UM	Water type SC_1, values of parameters
PH		8.42
Conductivity	µs/cm	1061
Alcalinity p	mval/L	0.1
Alcalinity m	mval/L	3.3
Total Hardness	mval/L	8.3
Calciu Hardness	mval/L	3.0
Cloride, Cl^-	mg/L	117.01
Sulfate	mg/L	155
Solid matters	mg/L	2.75
Organic matters	mg/L	11.37
Iron	mg/L	0.073
Aluminium,	mg/L	0.0175
Nitrite, NO^2-	mg/L	<0.1
Nitrate, NO_3^-	mg/L	10
Phosphate, PO_4^{3-}	mg/L	0.046
Cuprum, Cu^{2+}	mg/L	<0.015
Zinc, Zn^{2+}	mg/L	<0.1

RESULTS AND DISCUSSION

In this paper, we have been used as organic inhibitors the following polymers: PASAC-1, PASP and PASAC-2. The inhibition activity analysis of these organic compounds was made by assuming that the mechanism of inhibition by organic molecules is chemisorptions and that the energetics of the corrosion process per se is unaffected by the addition of substituent on the parent compound.

The polarization behaviour of carbon steels mentioned above was studied through the plotting of the polarization curves obtained using the potentiodynamic method, finding the kinetic parameters of corrosion (especially the density of the corrosion current) and their comparison with the kinetic parameters from solutions with different concentrations of inhibitors.

The corrosion parameters were calculated on the basis of potentiodynamic potential-current characteristics in the Tafel region (E=E_{corr} ± 150mV) and the vicinity of the corrosion potential ((E=E_{corr}± 15mV) according to Mansfield's theory.

$$\log i_a = \log i_{corr} + \left(E_i - E_{corr}\right)/b_a \qquad (2)$$

$$\log i_c = \log i_{corr} + \left(E_{corr} - E_i\right)/b_c \qquad (3)$$

This equation corresponded to linear anodic and cathodic Tafel lines. Current density i_{corr} was determined by extrapolating the Tafel lines to E=E_{corr} or according to the Stern-Geary equation. This resulted in:

$$i_{corr} = b_a b_c / 2.303\left(b_a + b_c\right) R_p \qquad (4)$$

where R_p was the polarization resistance, defined as the tangent of a polarization curve at E_{corr}.

$$R_p = \left(\frac{\mathrm{d}E}{\mathrm{d}i}\right)_{E=E_{corr}} \qquad (5)$$

In the present paper when the values of E-E_{corr} are higher than 70mV, slight but significant changes in the anodic and cathodic Tafel slopes were found.

Figures 1-2 show a series of potentiodynamic polarization curves of two-carbon steels electrode in aerated industrial cooling water type SC_1 in absence and presence of different concentrations of PASAC-1, PASP and PASAC-2.

Table 3

Kinetic corrosion parameters of carbon steel OL-37+ X ppm **PASAC 1** +SC_1 at 25°C

Inhibitor) (ppm)	i_{corr} ($\mu A/cm^2$)	R_p $K\Omega/cm^2$	R_{mpy}	$P_{mm/year}$	K_g g/m^2h	E(%)	E_{corr} (mV)	b_a (mV)	b_c (mV)	θ
0	13.01	1.78	6.07	0.15	0.137	-	-513	110	-215	-
50	3.45	4.50	1.61	0.0408	0.0365	74	-502	87	-119	0.74
100	1.957	6.88	0.913	0.023	0.02	85	-316	89	-84	0.85
300	1.642	11.26	0.766	0.019	0.017	87	-393	121	-109	0.87
500	1.257	18.53	0.586	0.014	0.0133	90	-344	196	-114	0.90
800	1.02	20.76	0.476	0.012	0.0108	92.1	-418	135	-105	0.921
1000	1.330	15.93	0.620	0.015	0.014	89.7	-380	168	-126	0.897
3000	1.377	14.27	0.642	0.016	0.0145	89.5	-397	139	-104	0.895

Table 4

Kinetic corrosion parameters of carbon steel OL-37+ X ppm **PASP**+SC_1 at 25°C

Inhibitor) (ppm)	i_{corr} ($\mu A/cm^2$)	R_p $K\Omega/cm^2$	R_{mpy}	$P_{mm/year}$	K_g g/m^2h	E(%)	E_{corr} (mV)	b_a (mV)	b_c (mV)	θ
0	13.01	1.78	6.07	0.15	0.137	-	-513	110	-215	-
100	5.62	4.27	2.62	0.066	0.0595	56.8	-532	72	-95	0.568
300	2.663	7.76	1.24	0.0315	0.0281	80	-629	145.8	-136	0.80
500	2.817	7.17	1.31	0.033	0.0297	78.3	-646	136	-155	0.783
800	4.245	4.70	1.981	0.050	0.045	67.4	-667	105	-162	0.674
1000	4.232	5.23	1.975	0.050	0.0448	67.5	-498	141	-164	0.675
3000	2.99	7.68	0.928	0.023	0.021	72	-423	215	-85	0.72

Table 5

Kinetic corrosion parameters of carbon steel OL-37+ X ppm **PASAC 2** +SC_1 at 25°C

Inhibitor) (ppm)	i_{corr} ($\mu A/cm^2$)	R_p $K\Omega/cm^2$	R_{mpy}	$P_{mm/year}$	K_g g/m^2h	E(%)	E_{corr} (mV)	b_a (mV)	b_c (mV)	θ
0	13.01	1.78	6.07	0.15	0.137	-	-513	110	-215	-
100	4.24	4.34	1.978	0.05	0.0449	67.4	-526	100	-140	0.674
300	5.945	3.16	2.77	0.07	0.062	57	-563	95	-142	0.57
500	5.274	3.64	2.461	0.062	0.055	60	-547	97	-150	0.60
800	4.013	3.64	1.872	0.044	0.0425	70	-537	85	-105	0.70
1000	6.204	2.96	2.895	0.073	0.0657	54	-508	105	-127	0.54
3000	6.514	2.56	3.033	0.076	0.0684	50	-577	101	-141	0.50

The figures 1-2 show a series of potentiodynamic polarization curves for two carbon steel electrodes in a cooling water type SC1, in absence and presence of different concentrations of inhibitor.

Analysis of the polarization curves from figures 1-2 indicates that at low overvoltages, the Tafel relationship are followed, showing that both anodic and cathodic reactions are activation-controlled. At higher overvoltages a limiting current appears on the anodic and cathodic polarization curves showing that, the transport of ions towards the electrode surface becomes the rate-determining step (concentration polarization). Analyzing the cathodic polarization curves from figure1-2 it can be observed that, on the large range of the potential the carbon steel electrodes behave very close to a passive behaviour. Practically, we can say that, in this potential range the electrode surface is passivated. We consider that, in this potential range, the cathodic reaction is hindered by the oxide film (passive film) from the electrode surface. In this potential range takes place the oxygen reduction cathodic reaction according to equation:

$$\tfrac{1}{2}O_2+H_2O+2e \rightarrow 2HO^- \qquad (6)$$

After this like passive range potential the cathodic current increases again and this increasing is due to the hydrogen evolution.

From polarization curves obtained by potentiodynamic method were calculated all kinetic corrosion parameters which are given in tables 3-8.

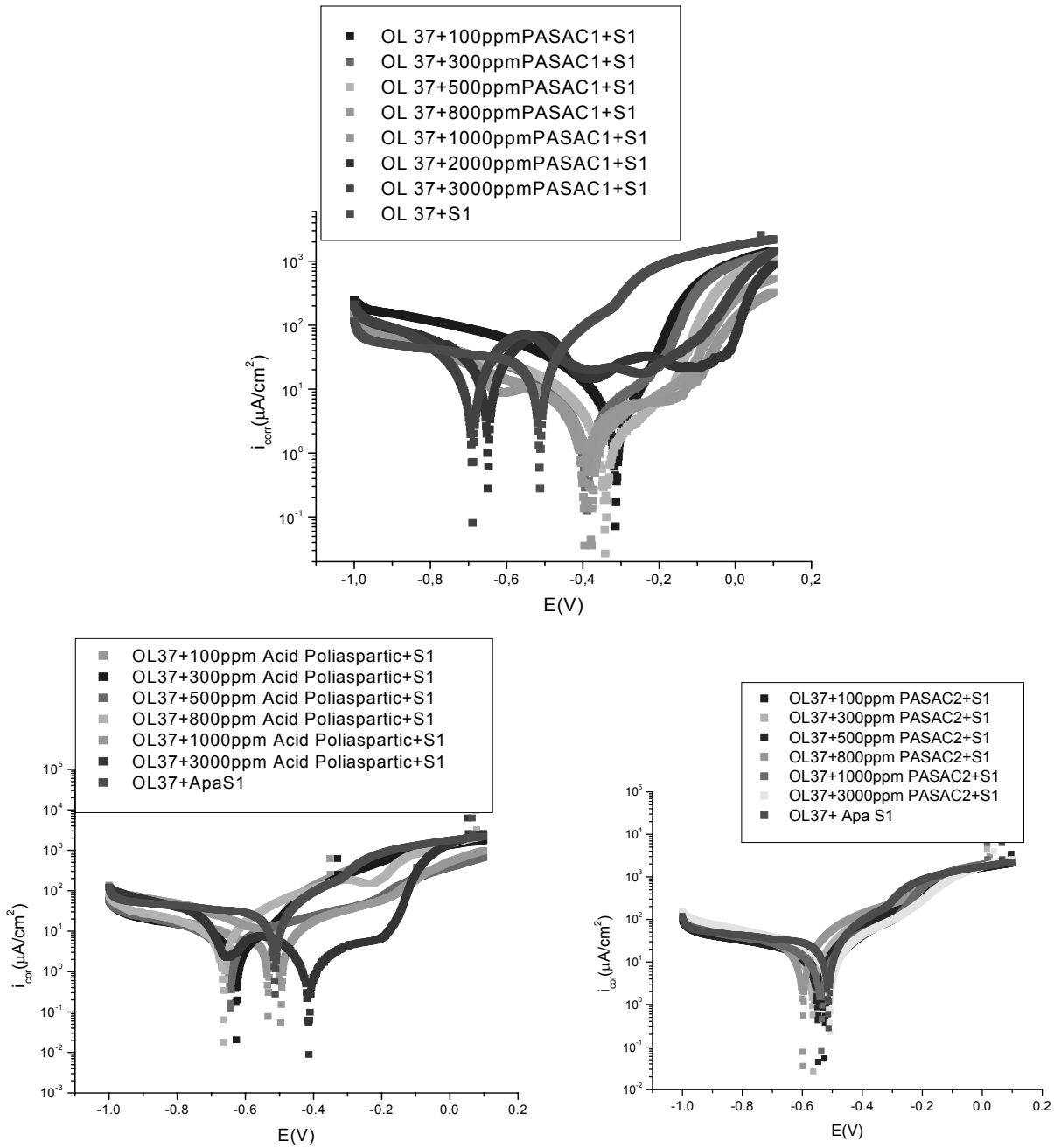

Fig. 1 – The polarization curves of OL-37 carbon steel in cooling water type SC1 in presence of PASAC1, PASP and PASAC2 organic inhibitors at 25 °C.

Table 6

Kinetic corrosion parameters of carbon steel OLC-45+ X ppm PASAC 1 +SC1 at 25°C

Inhibitor) (ppm)	i_{corr} (μA/cm^2)	R_p KΩ/cm^2	R_{mpy}	$P_{mm/year}$	K_{g_2} g/m^{2}h	E(%)	E_{corr} (mV)	b_a (mV)	b_c (mV)	θ
0	7.12	2.62	3.32	0.084	0.075	-	-414	91	-188	-
50	5.76	4.87	2.688	0.068	0.061	20	-461	100	-152	0.20
100	4.78	4.34	2.23	0.0566	0.05	33	-451	117	-148	0.33
300	1.201	16.92	0.56	0.014	0.012	83	-354	136	-120	0.83
500	1.069	20.02	0.498	0.012	0.011	85	-330	277	-105	0.85
800	1.68	14.86	0.784	0.019	0.0178	76	-435	106	-115	0.76
1000	1.91	11.63	0.891	0.022	0.020	73	-422	158	-180	0.73
3000	1.95	10.87	0.91	0.023	0.021	69	-424	147	-140	0.69

Table 7

Kinetic corrosion parameters of carbon steel OLC-45+ X ppm PASP +SC1 at 25°C

Inhibitor) (ppm)	i_{corr} (μA/cm^2)	R_p KΩ/cm^2	R_{mpy}	$P_{mm/year}$	K_g g/m^{2}h	E(%)	E_{corr} (mV)	b_a (mV)	b_c (mV)	θ
0	7.12	2.62	3.32	0.084	0.075	-	-414	91	-188	-
100	5.69	3.32	5.31	0.134	0.12	20	-524	101	-150	0.20
300	3.04	5.50	1.42	0.036	0.032	57.3	-514	95	-121	0.573
500	2.475	7.96	2.283	0.057	0.051	65.3	-457	125	-126	0.653
800	1.497	12.63	0.69	0.0176	0.015	78.9	-440	118	-115	0.789
1000	1.72	14.3	0.802	0.02	0.018	75.8	-493	176	-95	0.758
3000	1.97	9.87	0.92	0.024	0.022	72.3	-474	140	-120	0.723

Table 8

Kinetic corrosion parameters of carbon steel OLC-45+ X ppm PASAC 2 +SC1 at 25°C

Inhibitor) (ppm)	i_{corr} (μA/cm^2)	R_p KΩ/cm^2	R_{mpy}	$P_{mm/year}$	K_g g/m^{2}h	E(%)	E_{corr} (mV)	b_a (mV)	b_c (mV)	θ
0	7.12	2.62	3.32	0.084	0.075	-	-414	91	-188	-
100	6.78	2.99	3.26	0.083	0.074	7	-601	107	-205	0.07
300	6.09	3.35	2.84	0.072	0.064	16	-557	100	-183	0.16
500	5.584	3.06	2.60	0.066	0.059	22	-560	87	-153	0.22
800	5.32	3.48	2.48	0.063	0.056	26	-546	94	-152	0.26
1000	5.408	3.47	2.52	0.063	0.057	30	-547	107	-136	0.30
3000	5.650	3.31	0.81	0.073	0.072	21	-530	111	-150	0.21

Analyzing these tables, it can be observed that**,** the addition of the organic inhibitor to the amounts shown in the tables 3-8 leads in all the cases to inhibition of the corrosion process. This fact can be explained taking into account the effects of organic compounds on the electrochemical properties of the carbon steels in concordance with Donahue's theory.[14] It can be observed from tables 3-8 that, the inhibitor PASAC1 has a higher efficiency for corrosion system OL37+SC1 than for corrosion system OLC45+SC1. Analyzing in comparison the corrosion rate of organic inhibitors, in the same condition, one can see that, the PSAC-1 had a higher efficiency for corrosion system OL 37 and OLC 45 in SC1, PASP had a good efficiency for corrosion system OL 37 and OLC 45 in SC1 than PASAC-2.

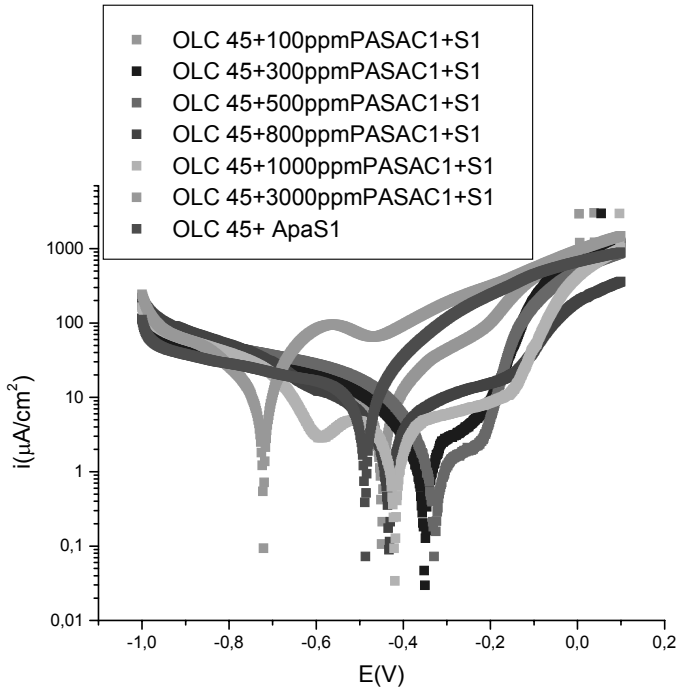

Fig. 2

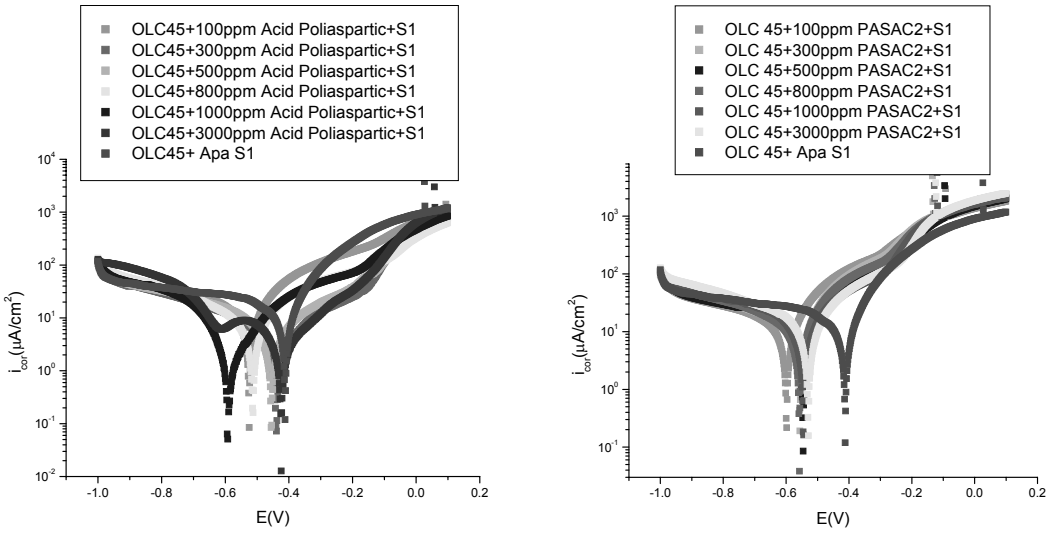

Fig. 2 –The polarization curves of OLC-45 carbon steel in cooling water type SC1 in presence of PASAC1, PASP and PASAC2 organic inhibitors at 25 °C.

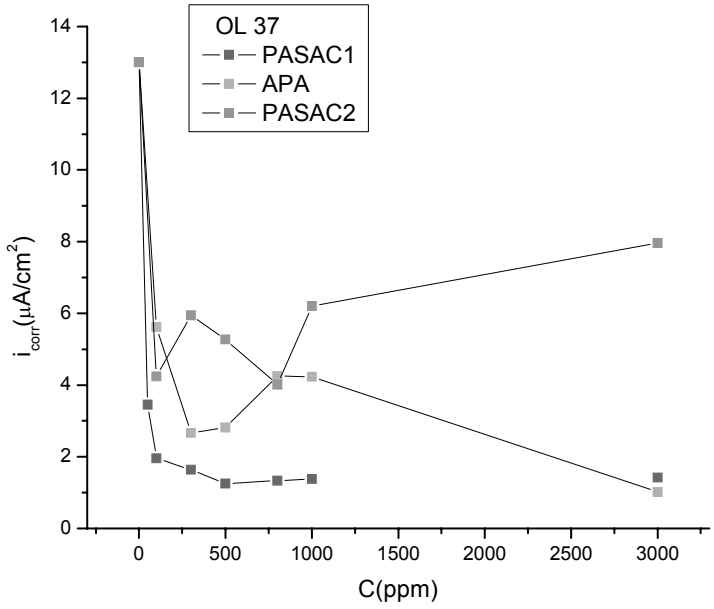

Fig. 3 –The influence of the inhibitor PASAC1, PASP and PASAC2 concentration on the corrosion rate of **c**arbon steel OL-37 in cooling water type SC_1 at 25^0C.

The variation curves of the corrosion current density function of the inhibitor concentration at different immersion times are presented in figures 3-4. From figures, one can see much better the influence of these parameters on the polarization behaviour of the two carbon steels in cooling water system**.**

We presume that, the higher inhibitor efficiency is a consequence of the stronger adsorption process. The molecules of organic inhibitor are adsorbed on the metal surface and form a barriere film, which hindered the corrosion process. To quantify the effect of inhibitor concentration on the corrosion rate, it is common to fit the rate data to equilibrium adsorption expression, such as Langmuir equation:

$$\theta/(1-\theta) = Kc \tag{7}$$

Where θ is the fraction of surface coverage by the inhibitor and K is the equilibrium constant for the adsorption reaction. θ is given by:

$$\theta = (i_{corr} - i_{corr.inhib})/i_{corr} \tag{8}$$

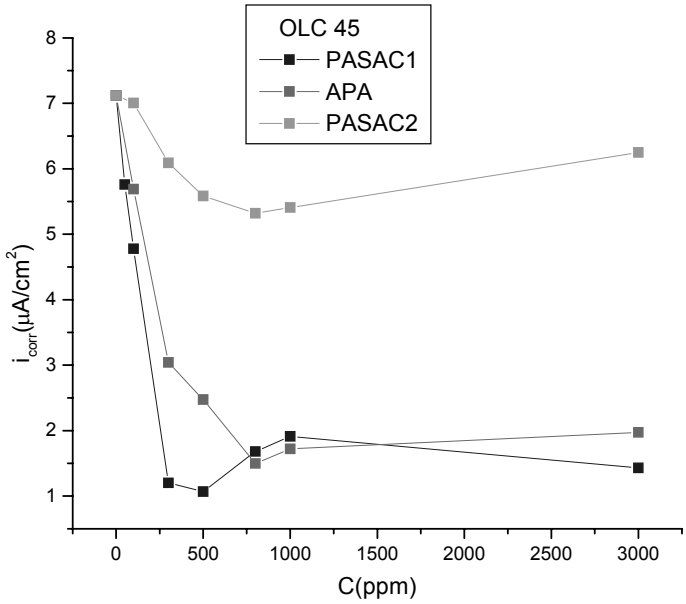

Fig. 4 – The influence of the inhibitor PASAC1, PASP and PASAC2 concentration on the corrosion rate of carbon steel OLC-45 in cooling water type SC1 at 25^0C.

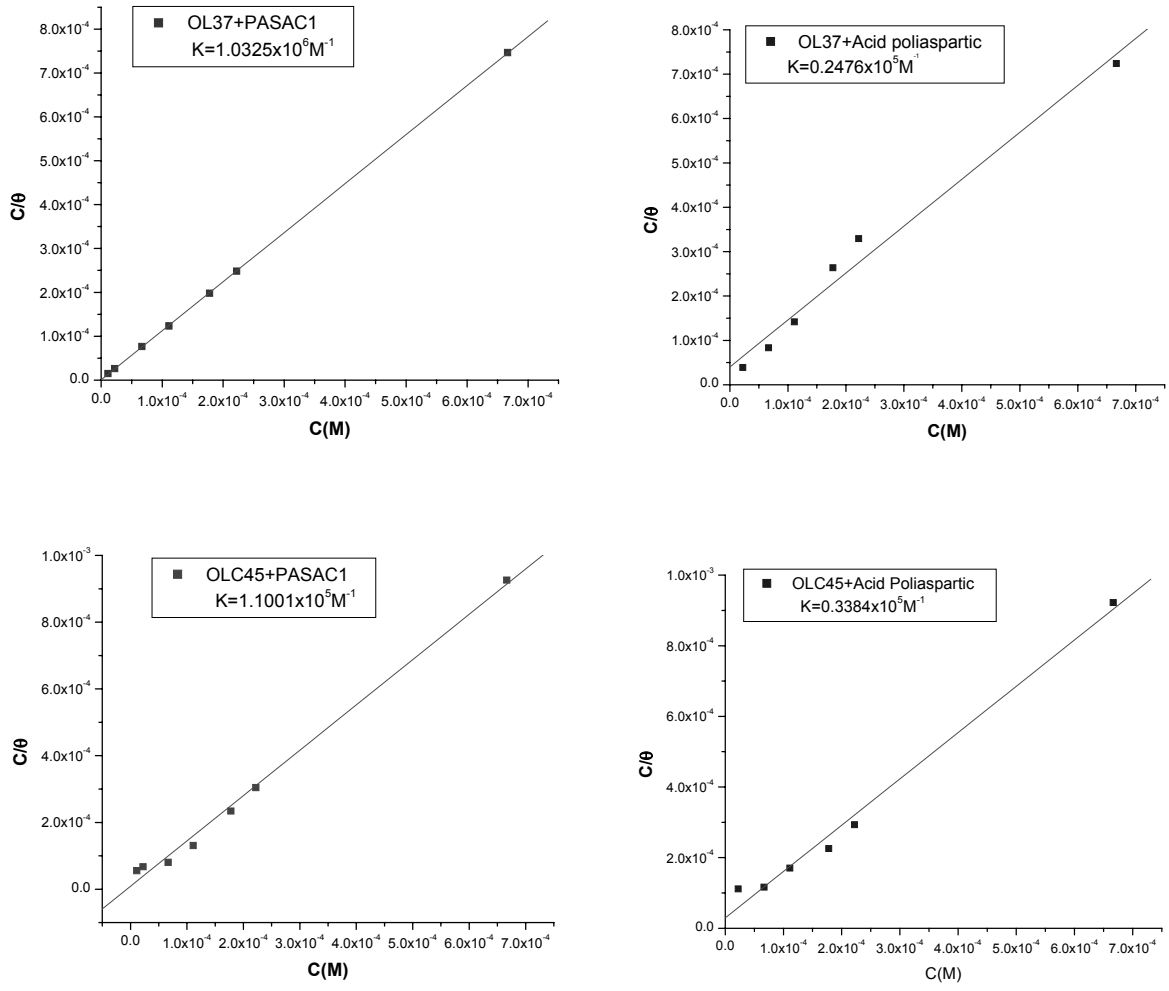

Fig. 5 – Langmuir plot for OL-37 and OLC-45 at different inhibitor concentrations.

Where $i_{corr, inh}$ and i_{corr} are the corrosion rates in the industrial cooling water SCS with and without inhibitor. Usage of the Langmuir treatment is often justified with the argument that inhibition must involve adsorption. In this paper, the Langmuir isotherm is rearranged to give:

$$c/\theta = c + 1/K \quad (9)$$

c/θ is plotted against c, when a linear relationship is obtained for organic inhibitor and a slope of near unity which indicates an approximate Langmuir behaviour . The adsorption equilibrium constants (K) for our corrosion systems are given in table 9.

These values of *K* point out the adsorption process of organic inhibitors on the electrode surface and consequently the decrease of the corrosion rate. Further, we shell try to show what kind type of adsorption process takes place on the electrode surface. The adsorption equilibrium constant (K_{ads}) is related to the standard free energy of reaction by the equation:

$$\ln K_{ads} = -\left(\Delta G_T^{\circ} / RT\right) \quad (10)$$

The obtained values ΔG_{ads}° up to -20Kjmol^{-1} are consistent with electrostatic interaction between the charged molecules (in our case, the inhibitor molecules) and the charged metal surface (physical adsorption), while those more negative than -40KJmol^{-1}, involve charge sharing or transfer from the inhibitor molecules to the metal surface to form a co-coordinative type of bond (chemisorptions see table 9).[28-30]

Table 9

The values of K_{ads} and ΔG_{ads}° for studied systems

The system	Type of metallic material	Values of K_{ads}, M^{-1}	Values of ΔG_{ads}° KJM^{-1}	Type of adsorption
Cooling water type SC_1+PASAC1	OL-37	1.0326x10^6	-34.291	Chemisorption and Physical adsorption
	OLC-45	1.1001 x10^5	-28.746	Chemisorption and Physical adsorption
Cooling water SC_1+Polyaspartic acid	OL-37	0.247x10^5	-25.054	Physical adsorption and chemisorption
	OLC-45	0.338x10^5	-25.827	Physical adsorption and chemisorption
Cooling water type SC_1+PASAC2	OL-37	0.1314x10^4	-17.784	Physical adsorption and chemisorption
	OLC-45	0.7704x10^4	-22.162	Physical adsorption and chemisorption

All spectra in these experiments were obtained at a resolution 4cm^{-1} in the region 4000-650 cm^{-1}.

In this paper, FT-IR spectrometry was used to identify whether there was adsorption and to provide new bonding information on the steel surface after immersion in the cooling water system containing organic inhibitor.[23-27]

The FT-IR spectrum of pure organic polymer PASAC 1 is show in figure 6a. A broad peak at 3278 cm^{-1} indicates the presence of the C-H bond of the PASAC1 and the appearance of the peak in region 1633 cm^{-1} and 1562 cm^{-1} corresponds to the C=O and N-H symmetric and asymmetric stretching vibration of the carbonyl group. The presence of C-N stretching frequency is clearly manifest in the region 1200 to 1020 cm^{-1}.

The transmission FT-IR spectra obtained for the carbon steel specimens (OL 37, OLC 45) immersed in cooling water systems type SC1 containing 500ppm PASAC1 inhibitor organic is presented in figure 6b. This shows the characteristics the bands for the adsorbed PASAC1 on the metal surface. A weak band in the range from 3217 cm^{-1}is attributed to C-H. The strong band approximately 1576 cm^{-1} is assigned to N-H symmetric stretching vibration. The peaks for C-N stretching modes can be assigned in the region around 1396 cm^{-1}.The bands 1100 cm^{-1} and 1060 cm^{-1} are attributed to C-O and C-N. Moreover, these FT-IR measurements indicated at 3800 cm-^{1} the direct bonding between Fe atoms and PASAC 1 molecules via O and N atoms, and the formation Fe-inhibitor complex and this reveal that there is only chemical adsorption occurred on the surface of the metal.

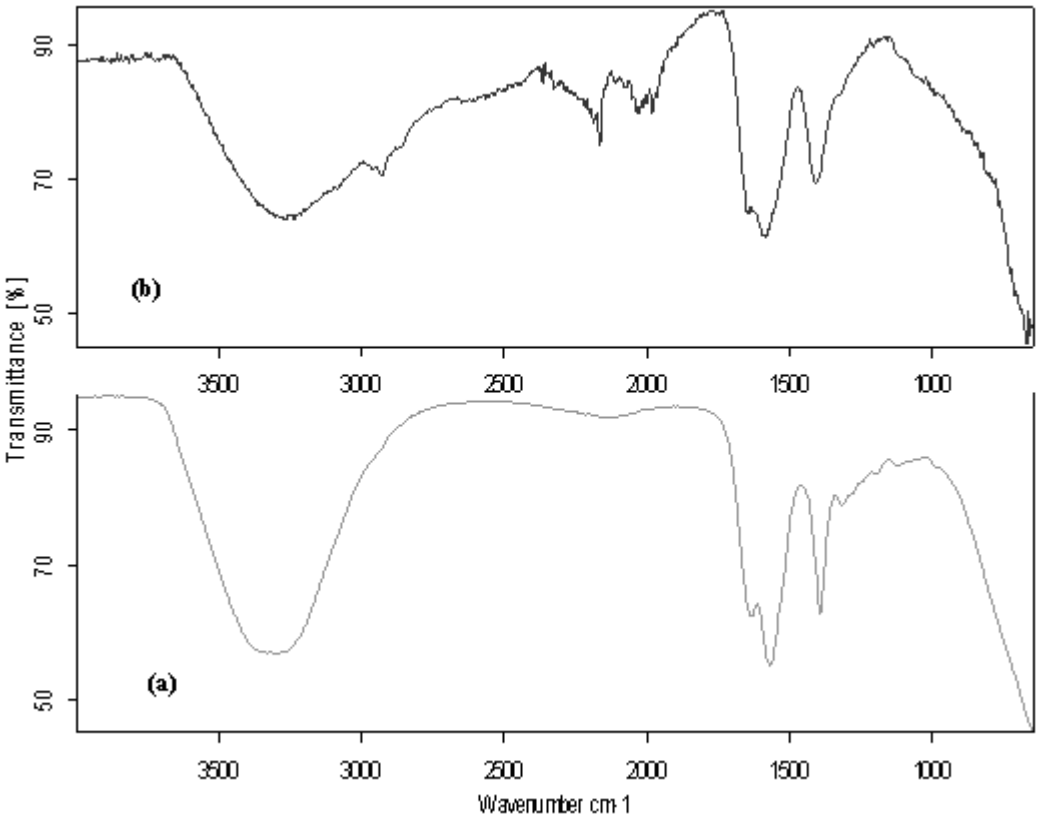

Fig. 6 – FT-IR spectra of (a) PASAC 1 and (b) OL 37+500 ppm PASAC 1 .

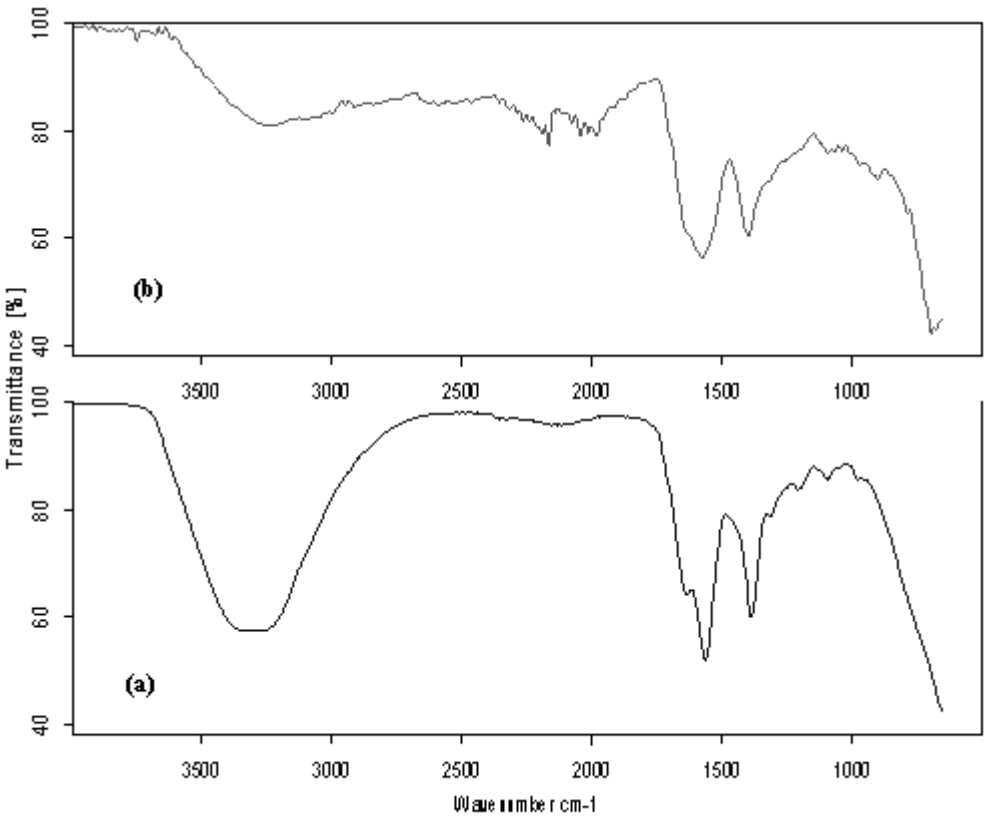

Fig. 7 – FT-IR spectra of (a) PASP and (b) OL 37+300ppm PASP .

The FT-IR spectrum of organic polymer Acid Polyaspartic (APAS) and of carbon steel immersed in cooling water SC1 containing 300ppm Acid Polyaspartic (APAS) is show in figure 7a and 7b. In the spectra of APAS, the characteristics peaks at 1192 and 3301 cm^{-1} correspond to the C-O and O-H stretching of the COOH, peak at 1636 cm^{-1} indicates the presence of the C=O, the band at 1571 cm^{-1} is assigned to the bending of N-H. The band at 1393 cm^{-1} is ascribed to the stretching vibration C-N. The weak band at 1200-1100 cm^{-1} is attributed to C-H bending. The FT-IR spectra of adsorbed protective layer formed on the surface after immersion in SC1 containing optimum concentration of inhibitor APAS is shown in figure 7b. As can be seen all important peaks in pure compounds appeared in adsorption layer on the metal surface. The band around 3270 cm^{-1} is attributed to O-H stretching, which indicates that the protective film contains H2O. The peak around 2918 cm^{-1} are assigned to C-H stretching vibration, the peaks at 1644 and 1583 cm^{-1} corresponds to the C=O and N-H symmetric and asymmetric stretching vibration. The presence of C-N, C-O is indicated by their starching modes at 1420 and 1125 cm^{-1}.This is already confirmed from the Langmuir adsorption isotherm studies.

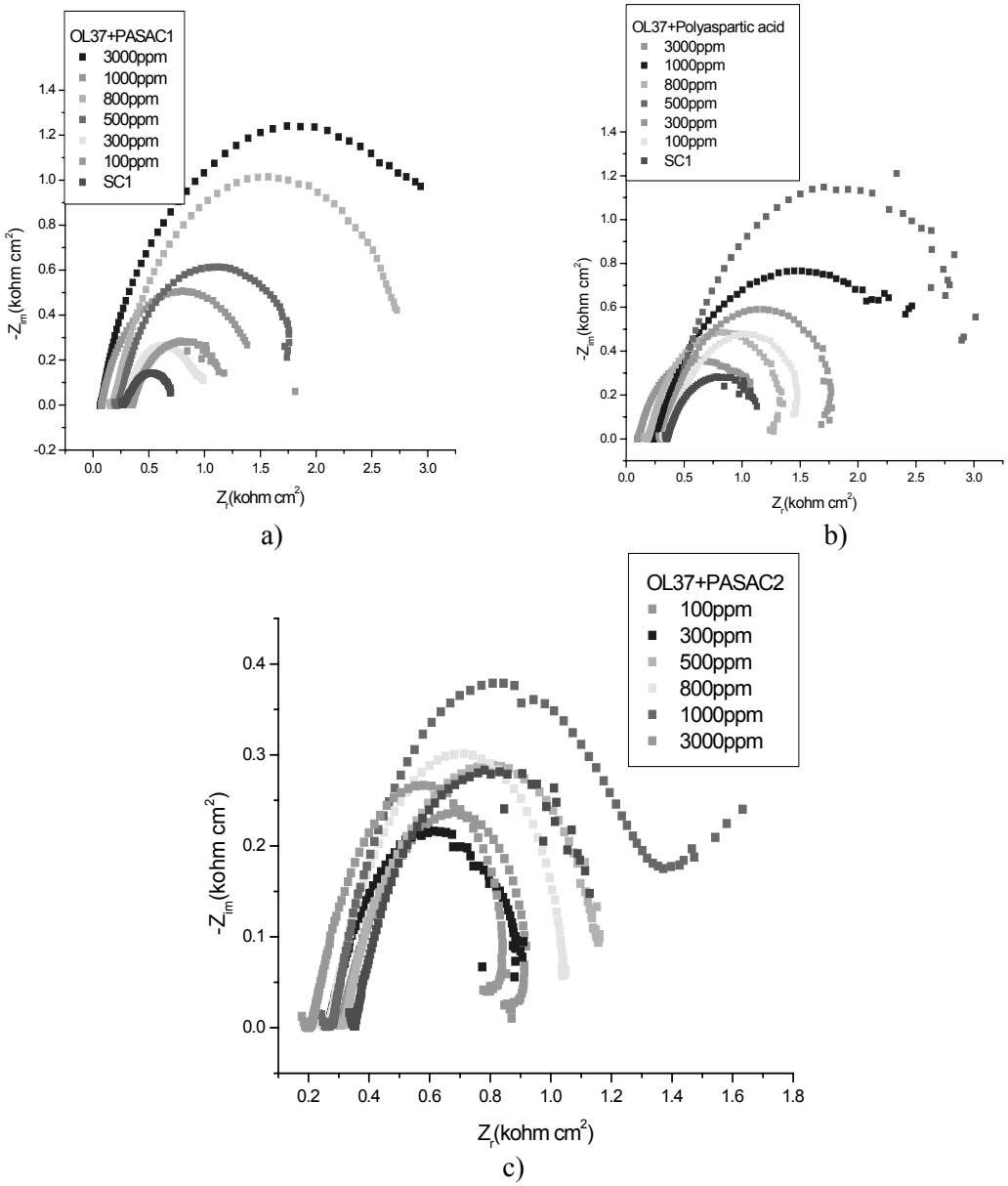

Fig. 8 – The Nyquist plot for OL 37 in $SC_1$with and without organic inhibitor at 25°C.

The corrosion of carbon steel in cooling water system SC1 in the absence and presence of PASAC 1, PASP and PASAC 2 were investigated by EIS at open circuit potential condition. Nyquist plots for carbon steel obtained at the interface in the presence of inhibitors at optimum concentration are given in figure 8 (a, b and c). All impedance spectra exhibit one capacitive loop and the diameter of the semicircles increases on increasing the inhibitor concentration suggesting that the formed inhibitive film was strengthened by the addition of inhibitors. However, these diagrams are not perfect semicircles which are attributed to frequency dispersion. The semicircular appearance shows that the corrosion of steel is controlled by charge transfer and the presence of inhibitor does not change the mechanism of dissolution. Figure also indicates that the diameters of the capacitance loops in the presence of PASAC 1, PASP and PASAC 2 are bigger than that in the absence of organic inhibitors, suggesting that PASAC-1 PASP and PASAC-2 has good anticorrosion performance on the carbon steel in SC1.

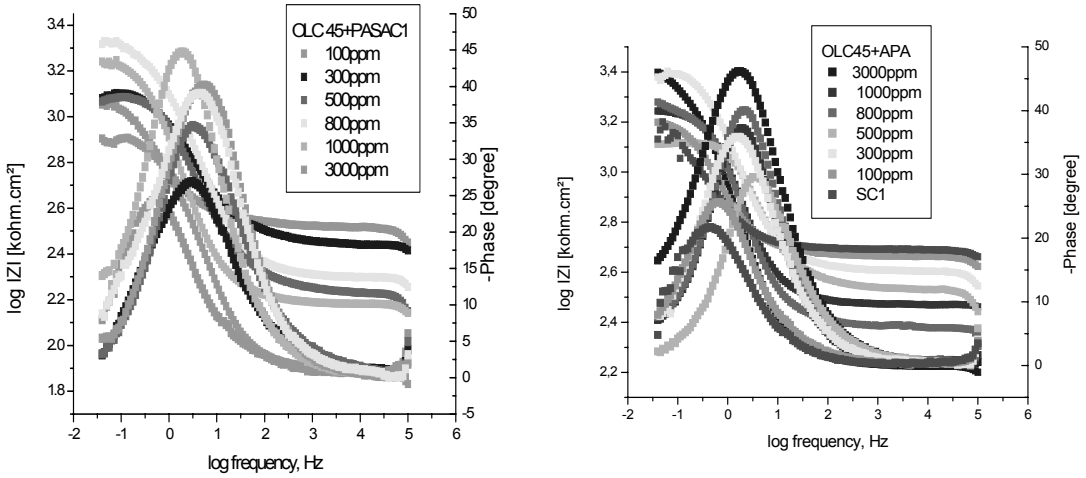

a) b)

Fig. 9 – The Bode plot for OLC 45 in $SC_1$with and without organic inhibitor at 25^{o}C.

All the obtained plots show only one semicircle and they were fitted using one time constant equivalent mode with capacitance (C), the charge transfer resistance (R_{ct}) and Rs solution resistance..

The corresponding Bode plots and shown in figure 9a and 9b.The lower capacitance value for SC1+OLC 45 with PASAC 1 and APAS, medium indicates the inhomogeneity of surface of the metal roughened due to corrosion The Cdl values decreases on the increasing the inhibitor concentration and reaches very low value for the optimum concentrations of all the studied systems indicating that the reduction of charged accumulated in the double layer due to the formation of adsorbed inhibitor layer.

Further, using the metallographic microscope the electrode surfaces were analyzed before and after a certain immersion in SC1. In figure 10 are given a few micrographies obtained by us for the following systems: carbon steel OL 37 and OLC-45 before and after a certain immersion in cooling water type SC1 with and without organic inhibitor. As it can be observed from figures 10 the corrosive attack is more accentuated in the cooling water system where the organic inhibitor concentration is lower than in the cases for which the organic inhibitor concentration is higher (see in comparison the micrographies from figure 10).

Analyzing in comparison the figures 10b, 10c, 10e and 10g, it can be observed that, on the surface of micrographies there are the adsorbed films of inhibitor and corrosion products and that, these films are thicker if the inhibitor concentration are higher. These films behave like a barrier between corrosive medium and metal surface and as a consequence the corrosion process is inhibited - see in comparison the figures 10. Analyzing in comparison the figures 10b and 10c, it can be observed that, the corrosive attack is much more accentuated in the case of OL 37+ water type SC1 system than in the case of OL-37+ water type SC1 +300ppm PASAC1 system. The same behaviour was observed for OLC 45(see in comparison figures 10i and 10j). This finding is in good concordance with the results obtained by electrochemical method (see tables 4 and 5) and the polarization curves from figures 1 and 2.

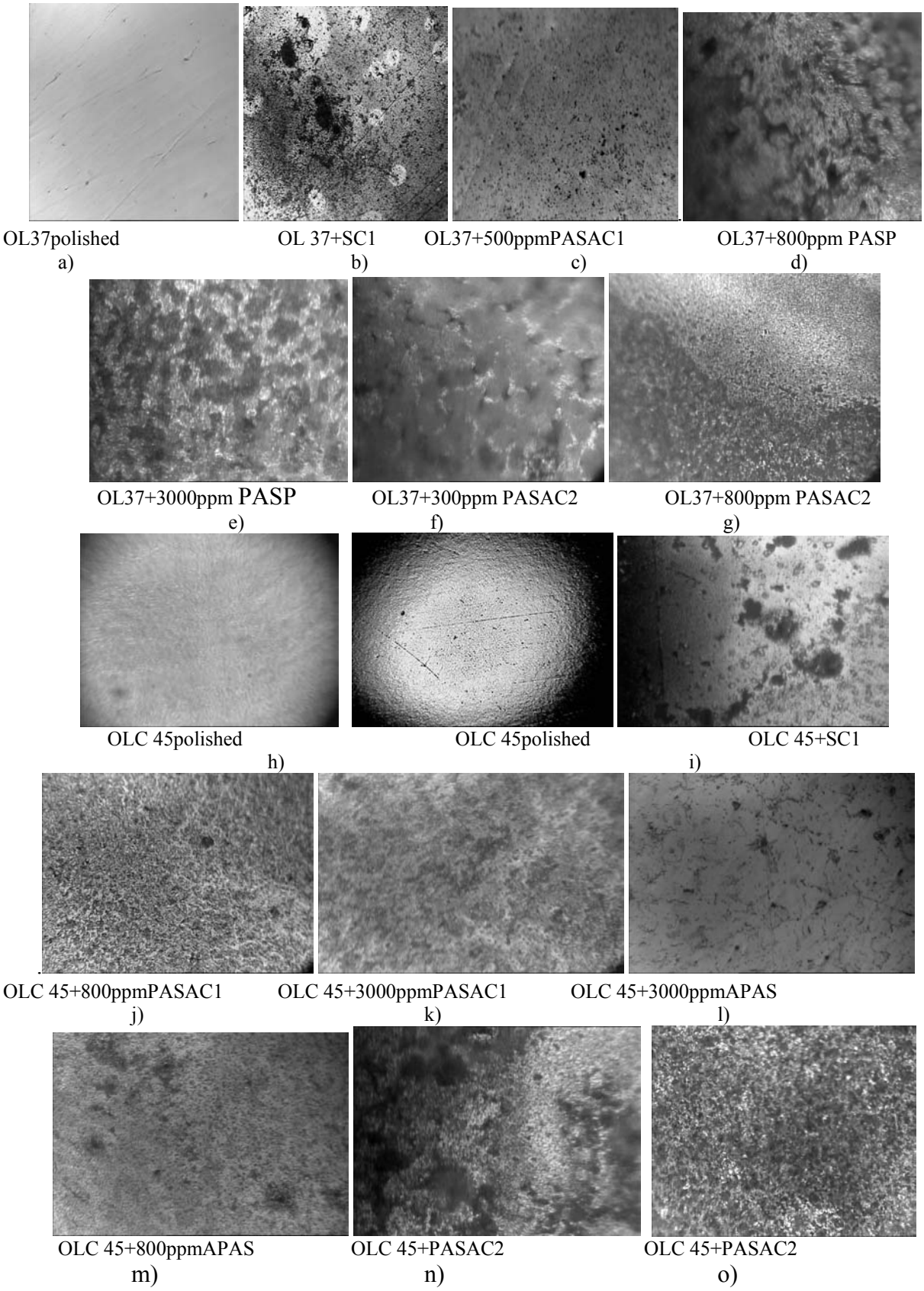

Fig. 10 – Micrographies of the carbon steel OL 37 and OLC-45 in cooling water type SC1 with and without organic inhibitor PASAC-1, APAS and PASAC-2.

CONCLUSIONS

In the studied corrosion systems at low over-voltages, the corrosion process is under activation control, while at high overvoltages is controlled by diffusion.

The addition of organic inhibitors led in all the cases to the inhibition of the corrosion process.

The new organic polymers which were obtained by us have presented a good inhibitory action and a significant efficiency for decreasing of the rate corrosion.

The organic inhibitors were adsorbed on the carbon steel surface according to a Langmuir isotherm. The values of the adsorption constant determined from the plot of Langmuir isotherm pointed out that, in these cases there is a mixture of physical and chemical adsorption of organic inhibitors.

The adsorption of the organic inhibitors at the electrode surface leads to the formation of an adsorbed organic molecules layer, which stabilizes the oxide passive film and in this way, the corrosion process is inhibited.

The inhibitor PASAC-1 had a higher efficiency for corrosion system OL-37 in cooling water type SC_1 than for corrosion system OLC-45 in the same cooling water SC_1.

In the cooling water SC_1 without inhibitors, the carbon steel OL-37 had a higher corrosion rate than the carbon steel OLC-45.

The corrosion rate of both carbon steels decreases if the inhibitor concentration increases up to a certain value and then, the corrosion rate increases again if the concentration of the organic inhibitor increases further.

In all of the cases, the organic inhibitor type PASAC-1 had a higher efficiency, APAS had a good efficiency than the organic inhibitor type PASAC-2.

Acknowledgments: Financial support from National research Grant PN-II-32-137/2008 (Roumanian Ministry of Education and Research/CNMP) is gratefully acknowledged.

REFERENCES

1. H. H.Uhlig and R.W.Revie, "Corrosion and Corrosion Control", Whiley, New York, 3rd edition., 1985.
2. D. Jones, "Principle and Prevention of Corrosion", MacMillan Publishing Company, New York, 1992.
3. K. C.Pillai and R.Narayan, *J.Electrochem.Soc.* **1978,** *125*, 1393.
4. J. L. Rozenfeld, "Corrosion Inhibitors", McGraw-Hill, New York, 1981, p. 109.
5. V. Branzoi and F. Branzoi, *Rev. Roum. Chim*., **2002**, *47*, 1193-1203.
6. D. P. Schwensberg and V. Ashworth*, Corros.Sci*., **1988**, *28*, 539.
7. V.Branzoi, F. Branzoi and L.Pilan, *Mater. Chem. and Phys.*, **2009**, *118*, 197-202.
8. T. Hirai, J. Yamaki, T. Okada and A. Yamagi, *Electrochim. Acta*, **1985,** *30*, 61.
9. D. G. Leaist, *J. Chem. Soc. Faraday Trans*., **1990,** *86*, 3487.
10. E. Kamis, F. Bellucci, R.M. Latonision and E. S. H. El-Ashry*, Corrosion* **1991,** *47*, 677.
11. M. Beier and J. W. Schultze, *Electrochim. Acta* **1992***, 37*, 2299.
12. F. Donahue and K. Nobe, *J. Electrochemical. Soc*. **1965,** *112*, 886.
13. Y.A.Aleksanyan, I.I.Rformatskaya and A.N.Podobaev, *Protection of Metals*, **2007**,*43*, 125-128.
14. E.M. Sherif and Su-Moon Park, *Electrochimica Acta*, **2006**, *51*, 4665-4673.
15. M.J Incorvia and S. Contarini, *J .Electrochem.Soc.*, **1989**, *136,* 2493.
16. F. Mansfeld, "Corrosion Mechanism", Marcel Dekker (Ed.), New York, 1987, p.119.
17. V.Branzoi, F. Branzoi and L.Pilan, *Molec. Crystal &Liquid Crystals*, **2006**, *446*, 305-318.
18. G Banerjee and S.N Malhotra., *Corrosion*, **1992**, *48,*10.
19. L.J.Antropov Proc. of The *1st International Congress of metallic Corrosion*, Butterworths, London **1962**, 147.
20. V. Brânzoi, A. Pruna and F. Brânzoi, *Rev Roum Chim*., **2007**, 52, 587-595
21. K. Aramaki, J.Uehre and H. Nishihare, *Proc. of the 11th International Corrosion Congress*, Florence, Italy, **1990,** *3*, 331.
22. G.B Hunt and A.K.Holiday, *Organic Chemistry* **1981**, *14*, 229.
23. R.D. Braun, E.E Lopez and D.P. Vollmer, *Corros. Sci*. **1993,** *34*, 1251.
24. H.W. Shen and Z.S Smialowskya., *Corrosion Sci*.**1989,** *45*, 720.
25. Loupy A., *Chemistry Today,* **2006,** *24*,.36.
26. Q.Qu, S.Jiang, W.Bai and L.Li, *Electrochim.Acta*, 2007, 52, 6811
27. Q.Quing, L.Li, S.Jing and Z.Ding*, J. Appl. Electrochem*., **2009,** *39*,569
28. M.F.L. Granero, P.H.L.S. Matai, I.V.Aoki and I.C.Guedes*, J.Appl.Electrochem*. **2009,** *39*,1199.
29. D. Gopi, K.M. Govindaraju and L. Kavitha, *J.Appl.Electrochem*., **2010,** *40*, 1349.
30. A. Prună, V. Branzoi and F. Branzoi**,** *Mater. and Technol.*, **2007,** *23*, 233-239.
31. V.Branzoi, F. Branzoi and F.Golgovici, *Mater. Chem. and Phys.*, **2003**, *78*, 122-131.